# Analysis of the effects of climate change on the gyre in Lake Biwa, Japan

Koue, Jinichi

Shimadera, Hikari

Matsuo, Tomohito

Kondo, Akira

# Journal of Hydroinformatics

# Analysis of the effects of climate change on the gyre in Lake Biwa, Japan

Jinichi Koue [iD] [a,b,]*, Hikari Shimadera[b], Tomohito Matsuo[b] and Akira Kondo[b]

[a] Graduate School of Maritime Science, Kobe University, 5-1-1 Fukaeminami, Higashinada-ku, Kobe, Hyogo 658-0022, Japan
[b] Graduate School of Engineering, Osaka University, 2-1 Yamada-oka, Suita, Osaka 565-0871, Japan
*Corresponding author. E-mail: koue@maritime.kobe-u.ac.jp, koue@ea.see.eng.osaka-u.ac.jp

[iD] JK, 0000-0003-2542-614X

## ABSTRACT

The currents of gyre (circulation) flow play an important role in the transportation and mixing of dissolved or suspended nutrients and chemical substances. In recent years, climate change has affected the flow field in Lake Biwa. However, how much climate change can influence the flow field has not been clarified enough yet. In the present study, using a three-dimensional hydrodynamic model, we investigated the effect of changes in air temperature, wind speed, and precipitation on the change of the flow field in Lake Biwa. For sensitivity analysis, numerical simulations were performed for a baseline case using realistic meteorological data from 2007 to 2012, as well as hypothetical cases using meteorological data. The analysis revealed that the changes in air temperature and precipitation changed stratification and vorticity in the surface layer in each season. The strength of the stratification affected the gyre strength in the surface layer. The change in wind speed, on the other hand, changed the wind stress acting on the lake's surface, influencing the strength of gyre significantly. Increased wind speed lengthened the radius of the gyre in Lake Biwa, while decreased wind speed made it weaker above and below the thermocline.

**Key words**: climate change, gyre, hydrodynamic model, Lake Biwa, structure of the stratification

## HIGHLIGHTS

- The currents of gyre flow play an important role in the transportation and mixing of dissolved or suspended nutrients and chemical substances.
- The significant feature of the flow field in Lake Biwa, Japan is the system of several gyres formed in the surface layer of the lake.
- The change in wind speed altered the wind stress acting on the surface of the lake, which significantly influenced the strength of the gyre.

## 1. INTRODUCTION

The study of the flow field is essential for understanding the transport and dispersion of nutrients from river inflows and lakes. Advection and diffusion of water also affect the distribution of the sediment in large lakes, and the variation in water temperature is significantly influenced by the flow field in lakes (Vincent *et al.* 1991). Hydrodynamics in large lakes is complicated and can change on hourly, daily, and seasonal timescales (Fischer *et al.* 1979). Hydrodynamics in lakes includes gyres (horizontal circulations), overturning (vertical circulation), wind-driven currents, gravity currents, and periodic flows such as internal waves and inertial oscillations. Internal waves generated by wind and gravity currents produced by river flow are important factors related to changing the flow field in lakes (Morales-Mar'n *et al.* 2017; Chen *et al.* 2020) and contributing significantly to the transportation of materials in Lake Kinneret (Stocker & Imberger 2003; Shilo *et al.* 2007) and Lake Grevelingen (Haren 2019). The currents of gyre in particular play an important role in the transportation and mixing of dissolved or suspended nutrients and chemical substances in lakes and enclosed oceans (Dipper 2022).

Global warming (IPCC 2021) can cause a shift from dimictic lakes to monomictic lakes, resulting in insufficient vertical overturning in Swiss lakes (Vinna *et al.* 2021). In other instances, in Lake Constance (Germany), the overturning of water ordinally occurred once a year, but due to the prolonged increases in air temperature, overturning in winter has become insufficient in recent years, according to observations (Rhodes *et al.* 2017). Previous research has shown that thermal stability in lakes influences the inter-annual variation of winter bottom conditions (Peeters *et al.* 2002; Arhonditsis *et al.* 2004; Yoshimizu *et al.* 2010).

The water quality in Lake Biwa due to climate change has been deteriorating since the 1950s (Kumagai & Vincent 2003; Kumagai *et al.* 2021). The reason for the decrease in dissolved oxygen is considered to be the strengthening of stratification caused by climate change in recent years. Climate change, such as the increase in air temperature, the decrease in wind speed, and the decrease in precipitation over the last 30 years, is a contributing factor to changing the flow field in the lake (Woolway *et al.* 2021). In particular, the rise in air temperature and the decrease in wind speed weaken the mixing of the water mass and can be the cause of low oxygenation and water contamination in the bottom layer.

Lake Biwa is the largest freshwater lake in Japan, which is located in Shiga prefecture. It is approximately 64 km long from north to south and covers an area of 672 km$^2$. A total of 119 rivers drain from the surrounding mountains into Lake Biwa, and its main outlet is the Seta River, flowing into the Seto Inland Sea at Osaka Bay. Its average depth is approximately 41 m, and the deepest point is approximately 104 m. The total volume of water restoration is 27.5 billion m$^3$. The lake provides an abundance of aquatic life and industry for the surrounding area in Japan.

There are many kinds of flows in Lake Biwa in Japan, which have various spatiotemporal scales. Wind-generated internal waves in Lake Biwa have also been studied using field observations (Saggio & Imberger 1998), modal analysis (Shimizu *et al.* 2007), and numerical simulation (Kitazawa *et al.* 2010; Koue *et al.* 2018). Internal waves, as demonstrated by Kitazawa *et al.* (2010), influenced the transport of hypoxic waters in the flow field in Lake Biwa. Gravity currents on the sloping boundary appeared to contribute to the gyre in the surface layer and lead to the restoration of oxygen and rich nutrients in the deep waters of Lake Biwa, according to Fer *et al.* (2002) and Akitomo *et al.* (2009a, 2009b). This phenomenon could have an impact on the ecosystem of the lake (Brooks & Zastrow 2002; Livingstone 2008).

Realistic flow conditions are generated as a result of the complicated superposition and interaction of these flows, but the flow conditions show significantly different aspects depending on the water area, depth, and season. These flows play an important role in the transportation and mixing of dissolved or suspended nutrients and chemical substances horizontally and vertically. The gyre in Lake Biwa especially changes the horizontal and vertical transportation of nutrients, algae, and dissolved oxygen. Therefore, in order to understand the actual distribution of nutrients and dissolved oxygen, the mechanism of generation of gyre should be elucidated, and at the same time, how much the change of meteorological conditions contributes to the gyre in Lake Biwa needs to be clarified.

The currents of gyre especially play an important role in the transportation and mixing of dissolved or suspended nutrients and chemical substances in lakes and enclosed oceans. The gyres in Lake Biwa were reproduced by the three-dimensional hydrodynamic model (Akitomo *et al.* 2009a, 2009b; Kitazawa *et al.* 2010; Koue *et al.* 2018). In recent years, climate changes have had an impact on the flow field in Lake Biwa. The effects of climate change on the structure of the stratification in Lake Biwa were analyzed by Koue (2022), who showed that the effects of wind speed were stronger than those of air temperature and precipitation on the structure of stratification. The effects of climate change on the vertical material circulation were discussed previously, but those of climate change on the horizontal circulation have not been evaluated. There is little research about the effect of climate change on the gyre in Lake Biwa. How much each meteorological element can influence the gyre has not yet been clarified. Therefore, it is critical to quantify the effects of each meteorological element on the flow field. In the present study, we examined the effect of changes in air temperature, wind speed, and precipitation on the change of gyre in Lake Biwa in the surface layer by using a three-dimensional hydrodynamic model.
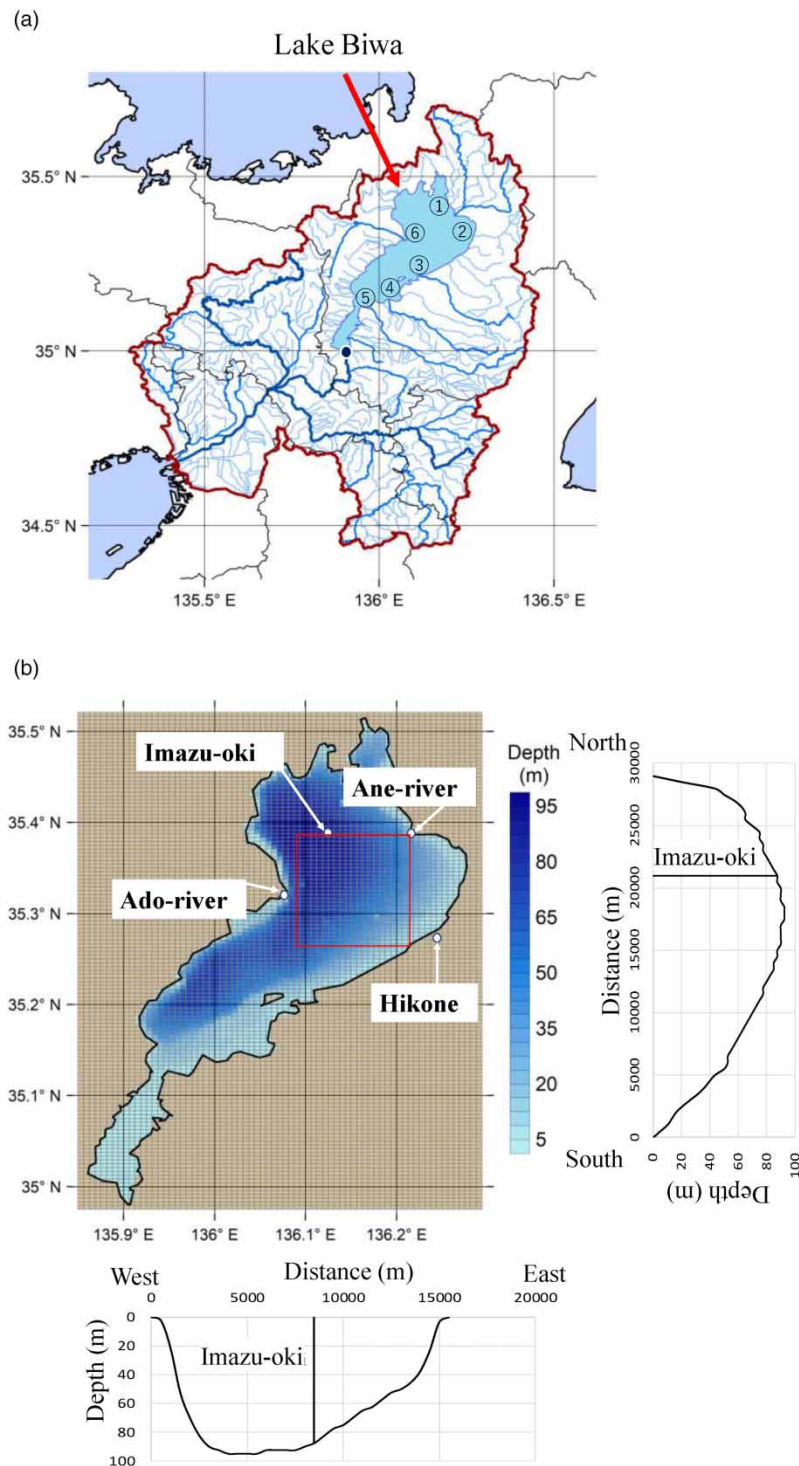
## 2. HYDRODYNAMIC MODEL IN LAKE BIWA

### 2.1. Study area

Figure 1(a) describes the surrounding river and the Yodo River Basin, with Lake Biwa as the upper reaches of the main river, covering an area of 8,240 km$^2$. Table 1 shows the flow rate of the main rivers which inflow into Lake Biwa. Figure 1(b) shows the calculation domain with the topography and water depth of Lake Biwa. The horizontal calculated domain is 36 km $\times$ 65.5 km with a grid size of 500 m. The vertical domain is 107.5 m, and the vertical grid size is 0.5 m from the surface to the 20 m depth of water and varies from 0.5 to 2.5 m as the water depth increases each 0.1 m in the vertical direction. This is to reproduce the change of water temperature in the surface layer more accurately.

### 2.2. The governing equations

In this study, the three-dimensional hydrodynamic model, developed by Koue *et al.* (2018), was used to figure out thermocline and vorticity in detail. This model was validated for reproducibility of the structure of the thermal stratification and flow field

**Figure 1** | (a) The surrounding river and the Yodo River Basin with Lake Biwa as the upper reaches of the main river and (b) calculation domain with the topography and water depth of Lake Biwa (the red square shows the region to calculate the vorticity). Please refer to the online version of this paper to see this figure in colour: http://dx.doi.org/10.2166/hydro.2023.075.

in Lake Biwa, compared with the observed data. The origin of the coordinate axes is in the southwestern edge of the domain on the horizontal plane. The $x$ and $y$ axes are set to west–east and south–north directions, respectively, and the $z$-axis directs upward.

**Table 1** | Flow rate of main rivers

|  | Name of river | Mean annual flow rate (m³ s⁻¹) |
|---|---|---|
| ① | Takatokigawa | 6.1 |
| ② | Anegawa | 22.3 |
| ③ | Echigawa | 13.0 |
| ④ | Hinogawa | 14.7 |
| ⑤ | Yasugawa | 32.4 |
| ⑥ | Adogawa | 21.2 |

Momentum equations ($x$ and $y$ directions) are written by:

$$\frac{\partial u}{\partial t} + u\frac{\partial u}{\partial x} + v\frac{\partial u}{\partial y} + w\frac{\partial u}{\partial z} - fv = -\frac{1}{\rho_0}\frac{\partial p}{\partial x} + \nu_h\frac{\partial^2 u}{\partial x^2} + \nu_h\frac{\partial^2 u}{\partial y^2} + \nu_z\frac{\partial^2 u}{\partial z^2} - \frac{g}{\rho_0}\int_z^0 \frac{\partial \rho}{\partial x}dz \tag{1}$$

$$\frac{\partial v}{\partial t} + u\frac{\partial v}{\partial x} + v\frac{\partial v}{\partial y} + w\frac{\partial v}{\partial z} + fu = -\frac{1}{\rho_0}\frac{\partial p}{\partial x} + \nu_h\frac{\partial^2 v}{\partial x^2} + \nu_h\frac{\partial^2 v}{\partial y^2} + \nu_z\frac{\partial^2 v}{\partial z^2} - \frac{g}{\rho_0}\int_z^0 \frac{\partial \rho}{\partial y}dz \tag{2}$$

The hydrostatic equation is given by the following equation:

$$0 = -\frac{1}{\rho_0}\frac{\partial p}{\partial z} - \frac{\rho}{\rho_0}g \tag{3}$$

The continuity equation is described by the following equation:

$$\frac{\partial u}{\partial x} + \frac{\partial v}{\partial y} + \frac{\partial w}{\partial z} = 0 \tag{4}$$

The conservation equation for water temperature is written by the following equation:

$$\frac{\partial T}{\partial t} + u\frac{\partial T}{\partial x} + v\frac{\partial T}{\partial y} + w\frac{\partial T}{\partial z} = \kappa_h\frac{\partial^2 T}{\partial x^2} + \kappa_h\frac{\partial^2 T}{\partial y^2} + \kappa_z\frac{\partial^2 T}{\partial z^2} \tag{5}$$

The density of water is calculated as follows (Fofonoff & Millard 1983):

$$\rho = 1,000.07 - 0.0469(T - 273.15)^2 - 0.0035(T - 273.15) \tag{6}$$

where $u$, $v$, and $w$ are the $x$, $y$, and $z$ components of current velocity (m s⁻¹), $T$ is the water temperature (K), $p$ is the pressure (N m⁻²), $\rho$ is the density of water (kg m⁻³), $\rho_0$ is the reference density of water ($= 10^3$ kg m⁻³), $g$ is the acceleration due to gravity ($= 9.8$ m s⁻²), $f$ is the Coriolis parameter ($= 8.34 \times 10^{-5}$ s⁻¹ corresponding to 35°N), $\nu_h$ is the horizontal eddy viscosity coefficient for momentum equations($= 1.0$ m² s⁻¹), $\kappa_h$ is the horizontal eddy diffusivity coefficient ($= 1.0$ m² s⁻¹), $\nu_z$ is the vertical eddy viscosity coefficient (m² s⁻¹) for momentum equations, and $\kappa_z$ is the vertical eddy diffusivity coefficient (m² s⁻¹). The horizontal eddy viscosity and diffusivity coefficients are chosen $1.0$ m² s⁻¹ as the constant values.

During summer, the thermocline was generally formed at the water depth from 10 to 30 m from the analysis of observed water temperature. This thermocline prevents the vertical transportation of momentum and heat fluxes. To take this effect into account, the parameter values of vertical eddy viscosity and diffusivity coefficients are estimated by using the Richardson

number. The Richardson number is calculated by the following equation:

$$Ri = -\frac{g}{\rho_0}\frac{\frac{\partial \rho}{\partial z}}{\left(\frac{\partial U_w}{\partial z}\right)^2} \tag{7}$$

where $U_w = \sqrt{u^2 + v^2}$ is the horizontal current velocity ($\mathrm{m^2\,s^{-1}}$), and the Richardson number is the dimensionless number that indicates the proportion of the buoyancy term to the flow gradient term as follows (Munk & Anderson 1948; Webb 1970).

Vertical eddy viscosity is given by the following equation:

$$\nu_z = \frac{0.0001}{(1.0 + 5.2Ri)} \tag{8}$$

Vertical eddy diffusivity is given by the following equation:

$$\kappa_z = \frac{0.0001}{(1.0 + \frac{10}{3} \times Ri)^{\frac{3}{2}}} \tag{9}$$

## 2.3. Initial conditions

As for the initial condition, the current velocity of each component $(x, y, z)$ was all set to be $0\,\mathrm{m\,s^{-1}}$. The initial conditions of water temperature were set to be the data on the 1st of April, which was linearly interpolated by using the observed data on the 20th of March and that on the 10th of April in the year 2006. The water temperature was observed by the Lake Biwa Environmental Research Institute twice a month at the monitoring point Imazu-oki as shown in Figure 1(b), the depth of which is 0.5, 5, 10, 15, 20, 30, 40, 60, 80, and 90 m.

The numerical simulation was carried out during the period from April 1st, 2006 to March 31st, 2012 within the spin-up period from April 1st, 2006 to March 31st, 2007. In the three-dimensional hydrodynamic model, the boundary conditions for the water volume and temperature of each river were assumed by the results, which were calculated by the hydrological model. By using this initial condition, the direction of the water flow, the current velocity, and the water temperature were calculated.

## 2.4. Boundary conditions

### 2.4.1. Meteorological conditions

The boundary conditions used were the same conditions described by Koue *et al.* (2018). Grid point value data from the Japan Meteorological Agency Meso-Scale Model (GPV MSM) were used to calculate the heat flux and wind stress on the water surface. The meteorological data were collected on air temperature, atmospheric pressure, wind direction and speed, and relative humidity. GPV MSM data had a spatial resolution of 0.0625° longitude by 0.05° latitude (horizontally 5 km) and a temporal resolution of 1 h. In order to reflect the GPV data into each mesh on the surface correctly, the meteorological data were given by interpolating the value which was averaged inversely proportional to the square of the distance. Since each data were updated every hour, it is possible to reproduce the heat balance and water flow on the surface of the lake. The air temperature and wind velocity at the Hikone Local Meteorological Observatory were used as the representative values in Lake Biwa. The location of the Hikone Local Meteorological Observatory is shown in Figure 1(b). Short-wave solar radiation was derived from hourly observation data at the Hikone Local Meteorological Observatory.

### 2.4.2. River condition

Taking the effect of the river inflow to Lake Biwa into account, not only the observed data but also the simulated data were given as boundary conditions. This is because the hydrodynamic model is assumed to be integrated into the Yodo River Basin Water System Model (Shrestha & Kondo 2015) in the future. The water temperature and the water volume, which were

calculated by the hydrological model, were interpolated each day for 56 rivers. The only outflowing river was located at the southernmost part of Lake Biwa. Furthermore, the grid size of the area of the simulation was 1 km, and the total number of meshes was 7,557. The data of the river inflow were updated every day for the analysis in detail. The location of six main rivers and the mean annual river inflow rates are shown in Figure 1(a) and Table 1. The total mean amount of annual river inflow rate was 177.5 m$^3$ s$^{-1}$.

## 2.5. Simulation cases

### 2.5.1. Baseline case simulation

The baseline case simulation was conducted for a period from April 1st, 2007 to March 31st, 2012 (Japanese fiscal year (JFY) 2007–2011) with a spin-up period from April 1st, 2006 to March 31st, 2007 using meteorological data derived from GPV MSM. The mean annual values of observed air temperature, wind speed, and precipitation at the Hikone Local Meteorological Observatory are shown in Table 2. The values of observed mean daily air temperature, wind speed, and precipitation data at Hikone are shown in Figure 2(a)–2(c), respectively. As described in Figure 2(b), the wind speed during autumn and winter was higher than other seasons. Seasonal mean values of them are indicated in Table 2. The periods from April to June, July to September, October to December, and January to March were set as spring, summer, autumn, and winter, respectively.

### 2.5.2. Hypothetical cases

Numerical simulations were carried out for a baseline case using realistic meteorological data from 2007 to 2012 and hypothetical cases using meteorological data with modified air temperature, wind speed, and precipitation for sensitivity analysis. For sensitivity analysis, the coefficients of variation ($\sigma/\mu$) were obtained from the mean value ($\mu$) and standard deviation ($\sigma$) of the mean annual air temperature, wind speed, and precipitation for 30 years from 1981 to 2010 at the Hikone Local Meteorological Observatory. The coefficient of variation ($\sigma/\mu$) was 0.21% for air temperature, 4% for wind speed, and 21% for precipitation. All pseudo-weather data were generated by multiplying $1 + \sigma/\mu$, $1 - \sigma/\mu$ by the air temperature, wind speed, and precipitation of GPV MSM data. The simulation cases named as AT + (AT−), WS + (WS−), and Pre + (Pre−) indicate the increase (decrease) in air temperature, wind speed, and precipitation, respectively. The pseudo-weather data of air temperature, wind speed, and precipitation data are shown in Table 2. The air temperature was calculated by the absolute temperature.

## 2.6. Evaluation of the strength of stratification and vorticity

The buoyancy frequency (Brunt–Väisälä frequency) is calculated to determine the strength of the stratification more precisely in each case in detail. The buoyancy frequency is a measure of stratification strength and is expressed in terms of the frequency $N$ of oscillations caused by buoyancy in a fluid under the influence of gravity and with density stratification. Since it is proportional to the square root of the vertical change in density, it is used as a parameter to represent the stratification strength.

The square of the buoyancy frequency is described as follows:

$$N^2 = -\frac{g}{\rho} \cdot \frac{\partial \rho}{\partial z} \tag{10}$$

**Table 2** | Mean annual values of observed AT, WS, and Pre at Hikone

| JFY | 2007 | 2008 | 2009 | 2010 | 2011 |
|---|---|---|---|---|---|
| AT (K) | 288.1 | 288.4 | 288.1 | 288.2 | 288.3 |
| WS (m s$^{-1}$) | 2.8 | 2.6 | 2.7 | 2.6 | 2.8 |
| Pre (mm) | 1,559.5 | 1,462 | 1,448.5 | 1,769 | 1,901.5 |
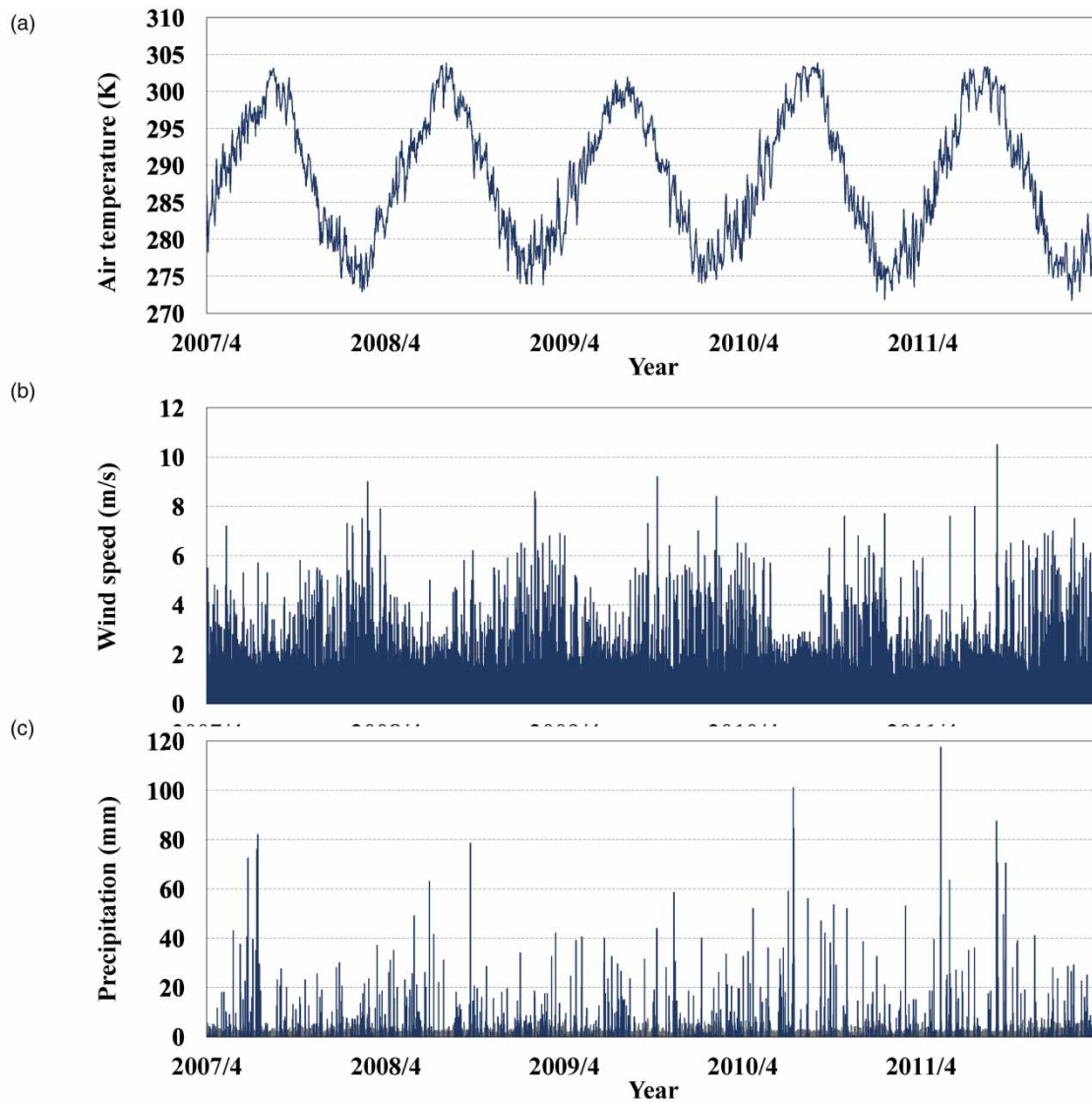
**Figure 2** | Time series of (a) air temperature, (b) wind speed, and (c) precipitation for meteorological conditions from JFY 2007 to 2011 at the Hikone Local Meteorological Observatory.

It is statically stable when $N^2 > 0$ and statically unstable when $N^2 < 0$. In order to determine the intensity of the gyre of Lake Biwa, the mean vorticity is used as follows:

$$\omega = \frac{\partial v}{\partial x} - \frac{\partial u}{\partial y} \tag{11}$$

$\omega > 0$ indicates the counterclockwise gyre, and $\omega < 0$ indicates the clockwise gyre.

## 3. RESULTS AND DISCUSSION

The present model reproduced the structure of stratification and the flow field in Lake Biwa based on the observed data approximately as indicated by Koue *et al.* (2018). The significant feature of the flow field in Lake Biwa, Japan is the system of the gyre formed in the surface layer of the northern part of the lake. A snapshot of the flow field in the surface layer at a water depth of 0.5 m is shown in Figure 3(a)–3(c). The flow field data in July 2008 was selected representatively since the gyre in the surface layer from spring to autumn was observed each year.
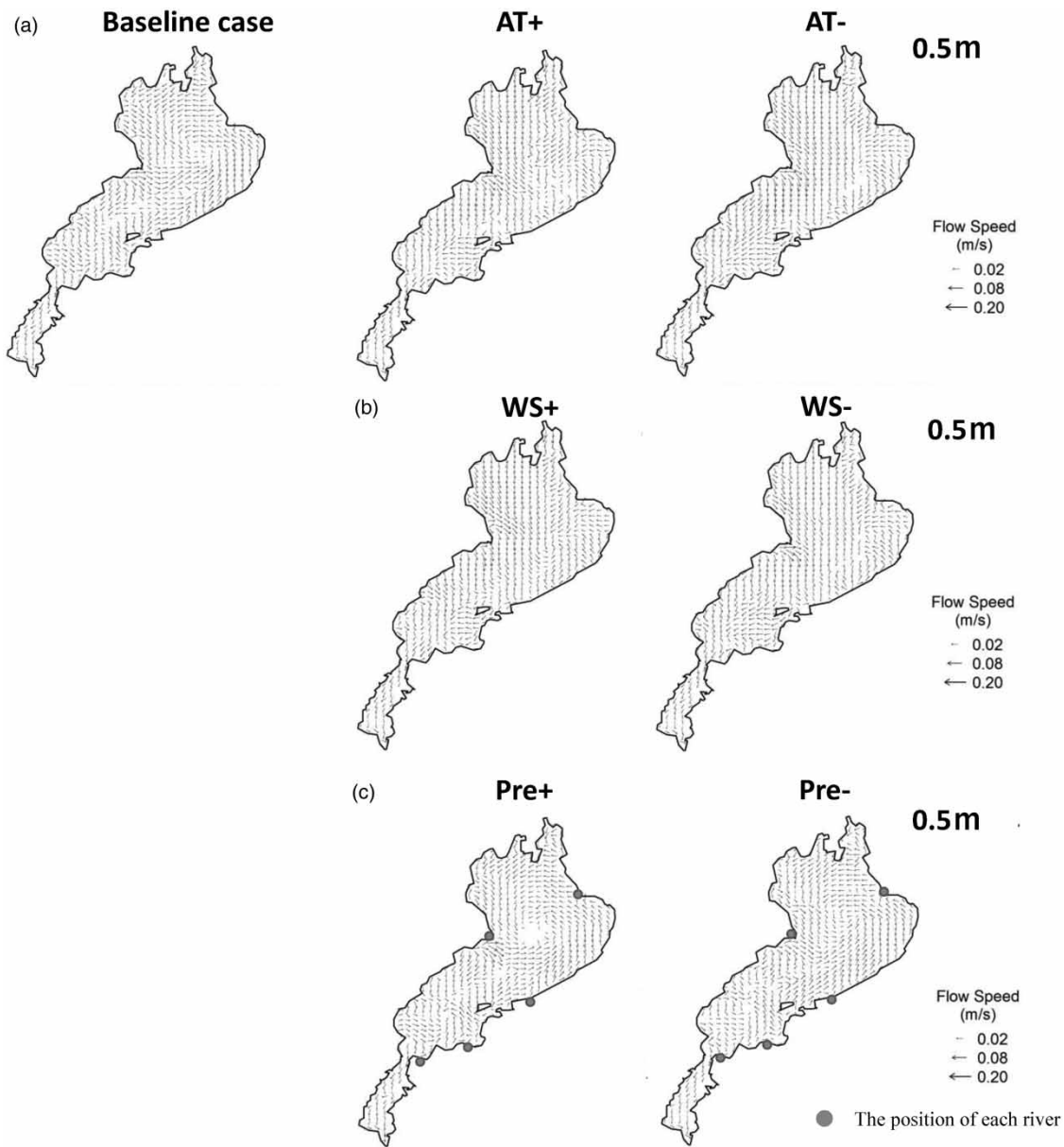
**Figure 3** | Flow field in the surface layer on July 23rd, 2008 at 12:00 baseline case and (a) air temperature, (b) wind speed, and (c) precipitation.

The first gyre appeared above the thermocline and existed from spring to autumn. The flow speed was approximately 10–30 cm/s, peaking in summer as shown in Figure 3. Since the 1980s, the details of the flow field have been clarified by the development of mooring equipment and flow velocity measuring equipment attached to the bottom of the ship. It was pointed out that the second and third gyres do not exist steadily and the first main gyre steadily exists according to the observation (Endoh *et al.* 1995; Kumagai & Vincent 2003) and simulation (Akitomo *et al.* 2009a, 2009b; Koue *et al.* 2018). These surface gyres were also observed in other large lakes (Rueda *et al.* 2009). Counterclockwise gyres have also been observed in Lake Michigan, Lake Superior, Lake Erie, Lake Constance, etc., and the gyre is affected by the shape of the basin, the difference in water depth, and the size of the lake (Bennington *et al.* 2010; Beletsky *et al.* 2013; Morales-Mar'n *et al.* 2017). In Lake Biwa, the effect of topographic heat storage effects is more pronounced due to the smaller gradient of the eastern shore.

There are two main causes of gyres in Lake Biwa: one is thermally driven and the other is wind-driven current. The first thermally driven one is also called the topographical heat storage effect. Due to the difference in the amount of heat storage in

the water column, a density gradient is formed, so that the flow is generated. In summer, water masses are less likely to warm up in deep water than in shallow water, and water masses with relatively low water temperatures accumulate offshore and have a relatively high density, so they sneak into the lower layers and serve as a compensation flow. As a result, a flow is generated from the coast to the offshore, and the Coriolis force acts on the right side of the northern hemisphere in the direction of travel, forming the first counterclockwise gyre.

As for the other wind-driven one, wind stress curl generates a counterclockwise gyre. In order for the first gyre to become a geostrophic current, the difference depending on the location of the wind direction must be a counterclockwise rotation by subtraction. Endoh *et al.* (1995) calculated the wind stress curl on Lake Biwa using meteorological observation data. It is reported that the wind stress curl tends to strengthen the first gyre in each season from spring to autumn. Once the gyre is formed, the geostrophic current is maintained even under the influence of the topographical heat storage effect, so it is difficult to quantitatively evaluate which the cause is.

The strength of the gyre was calculated by averaging the vorticity as described in Section 2.6. The increase and decrease in air temperature changed the stratification on the surface slightly (Figure 3(a)). Moreover, the increase and decrease in precipitation tended to strengthen and weaken the counterclockwise gyre on the surface, respectively (Figure 3(c)). The change in wind speed altered the wind stress acting on the surface of the lake, respectively, so that it significantly influenced the strength of the gyre. That is, the increase in wind speed made the radius of the gyre in Lake Biwa longer and the decrease in wind speed made it shorter both above and below the thermocline (Figure 3(b)).

The horizontal convergence of the lake water on the surface associated with the gyre plays an important role in the transportation of suspended nutrients and chemical substances. The flow speed of the gyre is a critical factor for the transportation of materials leading to the water environment. Therefore, it is important to maintain the gyre in Lake Biwa.

There is a main gyre in the northern part of Lake Biwa. The mean vorticity in the surface layer (0.5–10 m) in the northern part in each season is calculated in the region for a square with a side length of 12 km as depicted in Figure 1(b). The calculation results of mean vorticities are shown in Figure 4.

According to the analysis of mean vorticity in the northern part of Lake Biwa in the case of change of each meteorological element, in spring, at the beginning of stratification, the counterclockwise gyre began to form, and the increase in air
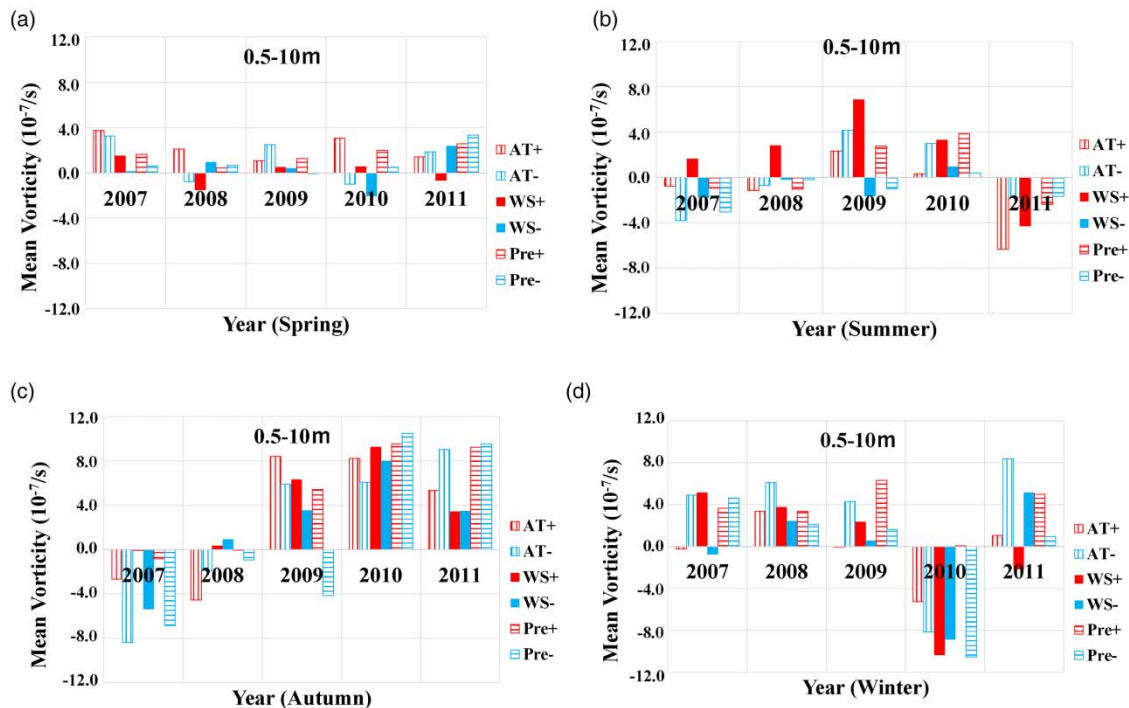


**Figure 4** | Difference of mean values of vorticity from the baseline case in the case of change of air temperature (AT +, AT−), wind speed (WS +, WS−), and precipitation (Pre +, Pre−) in the surface layer in (a) spring, (b) summer, (c) autumn, and (d) winter from JFY 2007 to 2011.

temperature and precipitation tended to strengthen the counterclockwise gyre (Figure 4(a)). The increase in air temperature enhanced the stratification, which made the counterclockwise gyre stable. The increase in precipitation increased the volume of inflow from the Ane River and the Ado River. The direction of each inflowing from the river into the lake created the counterclockwise flow, which enhanced the counterclockwise gyre. During summer, when the thermocline was formed, the counterclockwise gyre flow was weakened by fluctuations in air temperature and precipitation except in 2009 and 2010, and the increase in wind speed strengthened the counterclockwise gyre and the decrease in wind speed weakened the counterclockwise gyre except in 2011 (Figure 4(b)). In 2011, the wind stress curl in that summer season generated the clockwise flow; therefore, the increase in wind speed weakened the counterclockwise gyre. In autumn, as the air temperature decreased, the stratification weakened, and the strength of the counterclockwise gyre weakened (Figure 4(c)). In 2009, 2010, and 2011, the counterclockwise vorticity strengthened, while in 2007 and 2008, the clockwise vorticity strengthened with the change in air temperature, wind speed, and precipitation. In autumn 2007 and 2008, the wind speed was weaker than in other years, and the volume of precipitation was smaller than in other years (Figure 5).

In winter, the counterclockwise gyre flow was considered to remain in the case of the warm winter, while the clockwise gyre flow existed in the case of the severe cold winter. In fact, in the winter of 2010, the air temperature was cooler than usual, the wind speed was lower, and the amount of precipitation was less (Figure 5), resulting in a flow of snowmelt water from the coast to the bottom of the lake along the slope because the density of water in the coast was heavier than the surrounding water. Circulating currents formed from the lake center to the lakeshore but turned to the right under the influence of the earth's rotation in the northern hemisphere and the clockwise gyre occurred due to the topographical heat storage effect. Hence, only in 2010, a clockwise gyre flow was formed in the simulation (Figure 4(d)), and it was also observed in February 2011.

Under the thermocline, at the water depth of 20 m, the clockwise gyre was observed in the northern part of Lake Biwa in order to compensate for the counterclockwise gyre in the surface layer in the baseline case as shown in Figure 6. The increase and decrease in air temperature changed the gyre under the thermocline due to the strength of the stratification (Figure 6(a)). The increase and decrease in precipitation changed the counterclockwise gyre under the thermocline because the river inflow affected the flow field above the thermocline (Figure 6(c)). Depending on the strength of the counterclockwise gyre on the surface of the lake, it remarkably influenced the strength of the clockwise gyre under the thermocline (Figure 6(b)).

In order to analyze the relationship between the Brunt–Väisälä frequency and vorticity, the correlation diagram of mean change in the Brunt–Väisälä frequency and vorticity from the baseline case in the case of change of air temperature
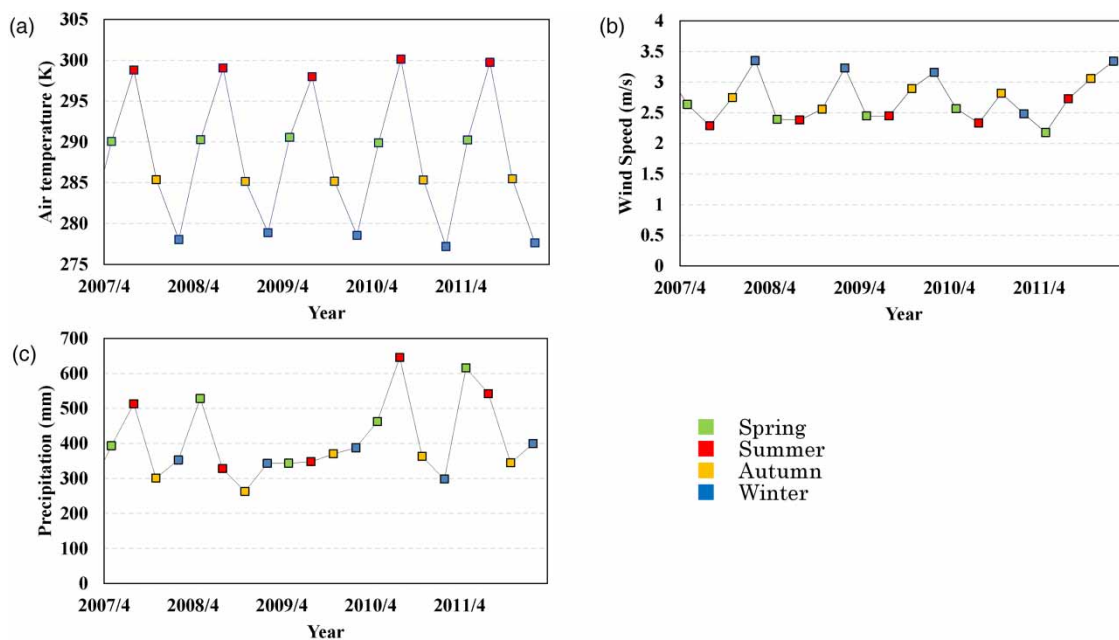


**Figure 5** | Seasonal changes of (a) air temperature, (b) wind speed, and (c) precipitation for meteorological conditions from JFY 2007 to 2011 at Hikone.
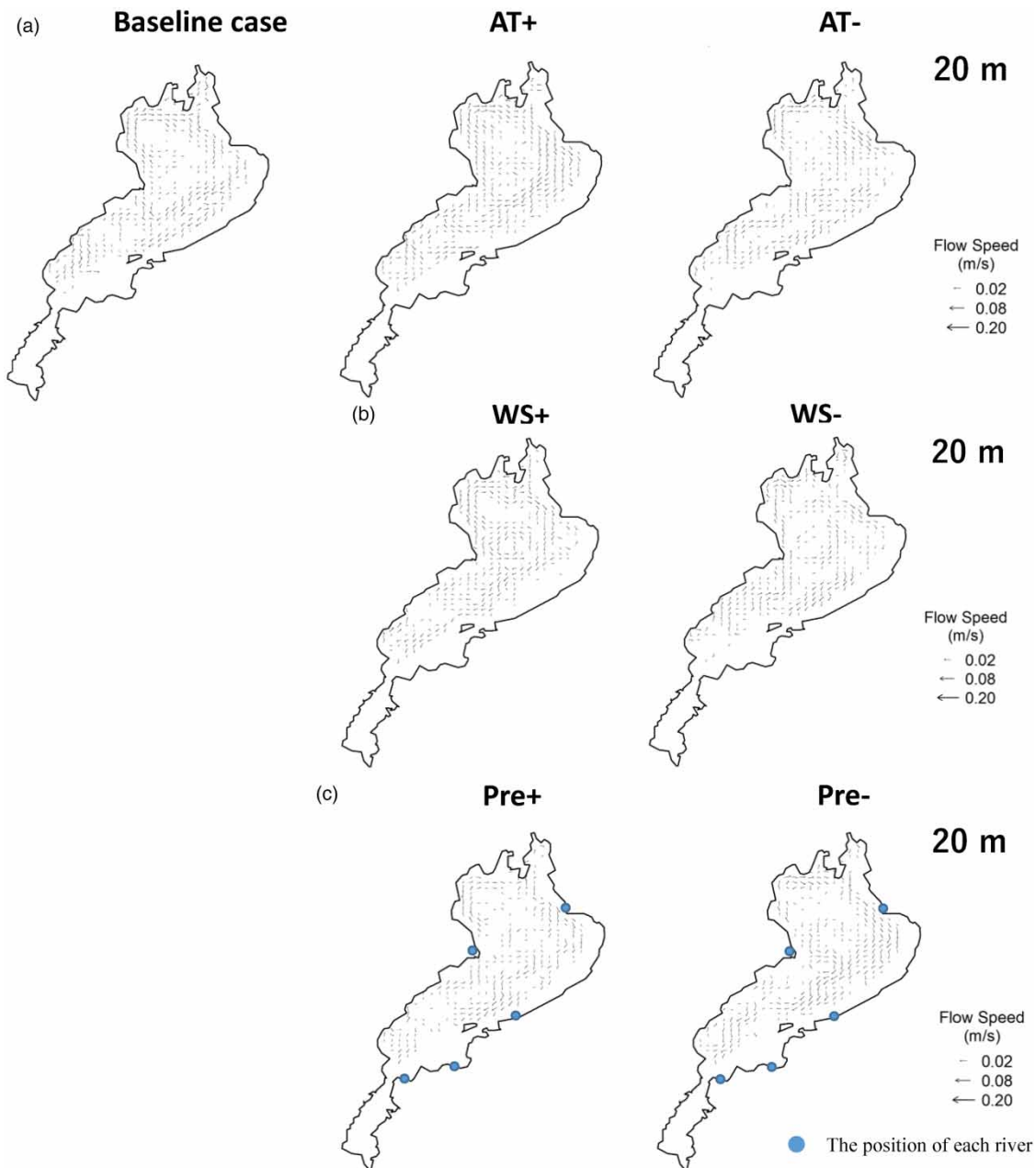
**Figure 6** | Flow field under the thermocline in July 23rd, 2008 at 12:00 baseline case and (a) air temperature, (b) wind speed, and (c) precipitation.

(AT + , AT−), wind speed (WS + , WS−), and precipitation (Pre + , Pre−) in the surface layer (0.5–10 m) (Figure 7(a)–7(d)), in the thermocline (10–30 m) (Figure 7(e)–7(h) ), and the deep layer (30–90 m) (Figure 7(i)–7(l) ) in each season from JFY 2007 to 2011 is shown in Figure 7.

In the surface layer, the Brunt–Väisälä frequency was positive with increasing temperature and decreasing wind speed during the spring when the stratification began, and the stratification was stable. For the vorticity, it took a positive value (approximately $2.0 \times 10^{-7}$) with increasing temperature and wind speed, thus strengthening the counterclockwise gyre. The change in air temperature and precipitation affected the counterclockwise gyre more than the change in wind speed. In summer, when the thermocline was stable, the Brunt–Väisälä frequency and vorticity had a wider range of values than in spring, and as wind speed increased, the Brunt–Väisälä frequency also became negative, the stratification was unstable,
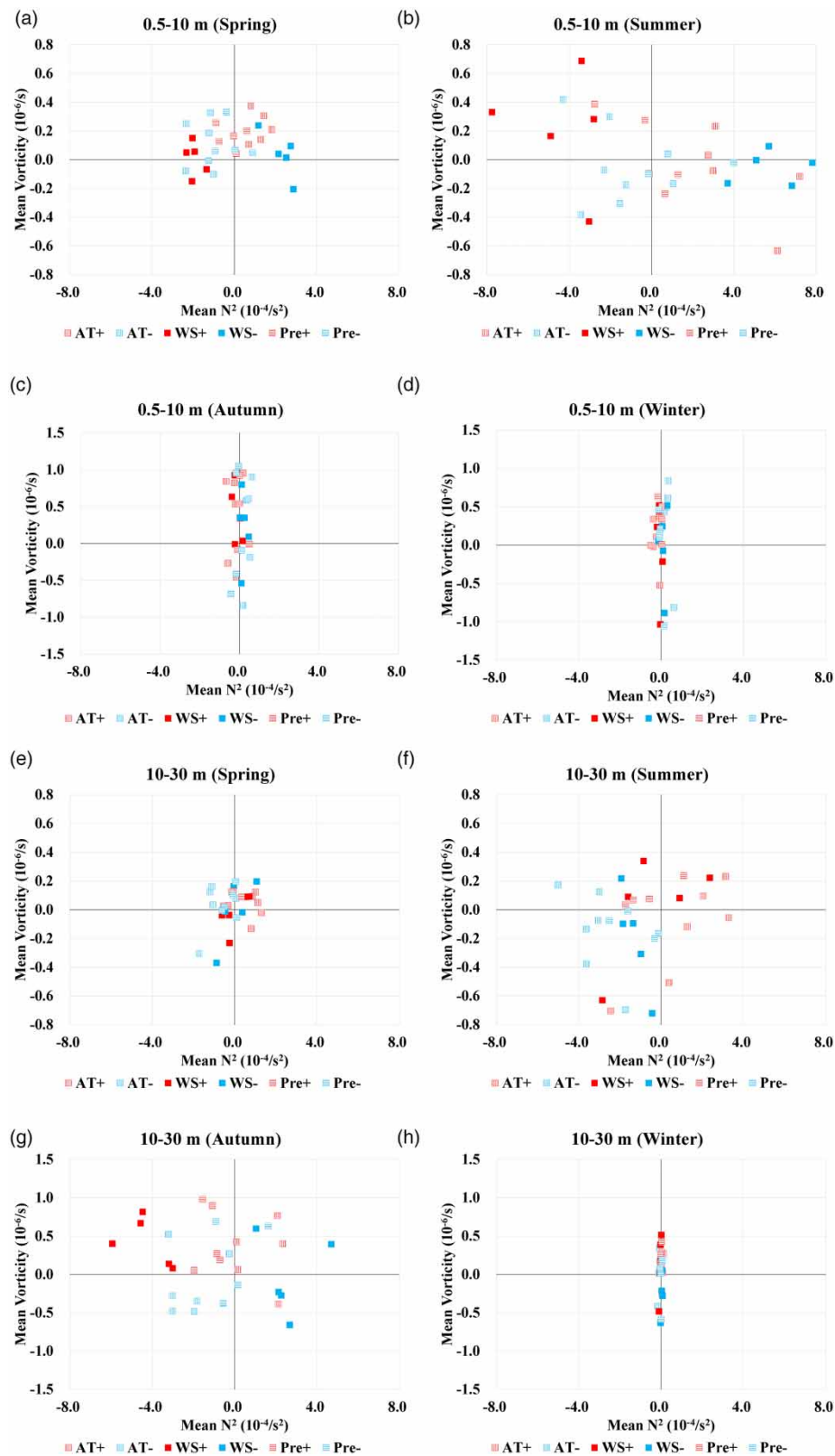
**Figure 7** | Correlation diagram of the mean change in Brunt–Väisälä frequency and vorticity from the baseline case in the case of change of air temperature (AT +, AT−), wind speed (WS +, WS−), and precipitation (Pre +, Pre−) in the surface layer (0.5–10 m) (a–d), in the thermocline (10–30 m) (e–h), and in the deep layer (30–90 m) (i–l) in each season from JFY 2007 to 2011. (*continued.*).
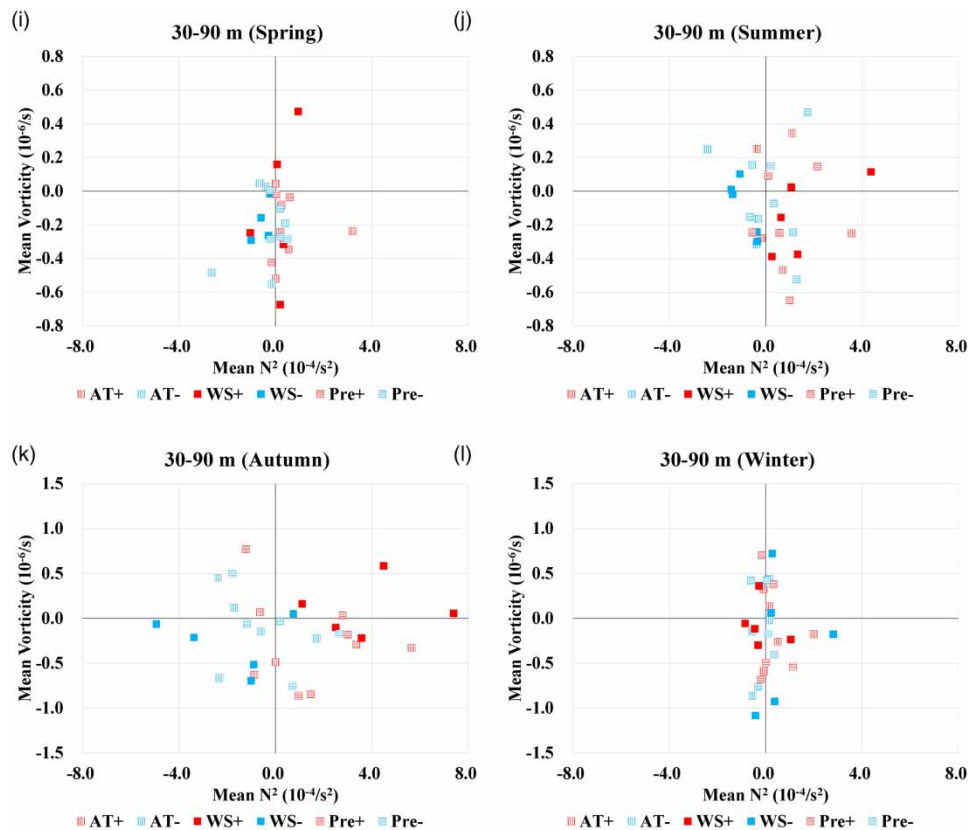
**Figure 7** | Continued.

and the counterclockwise gyre tended to be stronger. In autumn, when the air temperature decreased and stratification began to collapse, the order of the strength of vorticity increased from $8.0 \times 10^{-7}$ to $1.6 \times 10^{-6}$, which was approximately twice that of the summer season. The fluctuations in vorticity were large due to the change in air temperature, wind speed, and precipitation. In winter, when the entire layer was mixed, the vorticity tended to be negative and less than that in autumn.

In the thermocline, both vorticity and the Brunt–Väisälä frequency did not change much in spring due to the change in each meteorological factor unlike in the surface layer. In summer, the Brunt–Väisälä frequency was reversed, and vorticity tended to be similar to that of the surface layer because the stratification structure was stable. In autumn, the fluctuation of vorticity due to the change in each meteorological element was similar in the surface layer and the thermocline, and the Brunt–Väisälä frequency was more variable in the thermocline than in the surface layer. In winter, the surface layer and the thermocline showed almost the same level of fluctuation due to each meteorological element. In the deep layer, the direction of vorticity was opposite to that of the surface layer and the layer shallower than the thermocline, and the clockwise vorticity was stronger. In terms of changes in each meteorological element, from spring to summer, the increase in wind speed caused the stronger counterclockwise vorticity, while the decrease in wind speed caused the weaker counterclockwise vorticity. From autumn to winter, for each climatic factor, the order of the strength of vorticity increased from $8.0 \times 10^{-7}$ to $1.6 \times 10^{-6}$ in the deep layer as well as in the surface layer and the layer shallower than the thermocline, which was approximately twice as large as that in summer, and the flow tended to be opposite to that in the layer shallower than the thermocline.

The seasonal effects of air temperature, wind speed, and precipitation variations on the gyre in the lake are shown. In spring, as the stratification increased, the counterclockwise gyre occurred due to the topographical heat storage effect. The effect of air temperature change on the gyre was stronger than that of wind speed. In summer, when the thermocline was stable, the change in wind speed had a stronger impact on the gyre than changes in air temperature and precipitation. This indicated that the gyre was formed by the heat storage effect with the onset of stratification and that the wind curl continued to strengthen the gyre during the summer season. During autumn and winter, when stratification collapsed and vertical

mixing occurred, vorticity orders were approximately twice as large as in summer. In winter, the gyre tended to remain counterclockwise if the winter was warm at the surface and came to be clockwise if the winter was severe. Especially in winter, the inflow from snowmelt water influenced the strength of the clockwise gyre, depending on the strength of the vertical mixing. The gentle slope of the eastern shore of Lake Biwa made the snowmelt water fall down, which contributed to the clockwise gyre, and the intensity of it also depended on the strength of vertical mixing in all layers of Lake Biwa.

Nutrients and anoxic water masses produced by the decomposition of organic matter deposited on the lake bottom are diffused into all layers by vertical mixing in winter and then spread throughout Lake Biwa by the horizontal gyre flow from spring to autumn. When the eutrophication caused a red tide or blue-green algae bloom in a certain area, or if water pollution occurred when the wind speed was strong, the pollution would spread over a wide area due to the effects of the gyre currents. In the spring season, the strength of the currents is also affected by the air temperature and precipitation because of the strong thermal influence. At the depths below the thermocline, the flow in the opposite direction to that of the surface layer is formed, so meteorological changes have a significant impact on the material circulation. In summer, when the stratification is strong, the change in wind speed has a greater impact on the gyre than air temperature and precipitation; therefore, water pollution can affect a wider area.

## 4. CONCLUSION

In the present study, the analysis revealed that the change in air temperature had an effect on stratification in the surface layer, and as a result, the strength of the gyre in the surface layer changed. The difference in the water temperature in the horizontal direction and the difference in volume for advection–diffusion due to the amount of heat depending on the water depth affected the gyre flow. The change in wind speed, on the other hand, altered the wind stress acting on the lake's surface, which had a significant impact on the strength of gyre. Increased wind speed lengthened the radius of the gyre in Lake Biwa, while decreased wind speed made it weaker above and below the thermocline. The change in precipitation had an effect on the strength of the gyre because the direction of river inflow from the Ane River and the Ado River enhanced the counterclockwise gyre. The water temperature of rivers was a few degrees Celsius lower than that of Lake Biwa, which affected the flow field at depths below the thermocline.

The first gyre flow existed in the center of the circle in the northern part of the lake during a stratified season as the observational studies showed. In addition, in order to compensate for the flow field in the surface layer, the clockwise gyre existed right under the thermocline. The overall results would help to understand the movement of the substances in all layers of the lake. By analyzing the effects of climate change on the gyre of Lake Biwa, it is possible to figure out the flow field of Lake Biwa and track the movement of nutrients and suspended sediments. The intensity of the gyre has a remarkably important effect on the material cycle because the gyre can converge offshore of nutrients and flora and fauna plankton. Predicting the intensity of gyre due to climate change would play an important role in the conservation of the ecosystem of large lakes in the future.

## DATA AVAILABILITY STATEMENT

All relevant data are included in the paper or its Supplementary Information.

## CONFLICT OF INTEREST

The authors declare there is no conflict.

## REFERENCES

Akitomo, K., Tanaka, K., Kumagai, M. & Jiao, C. 2009a Annual cycle of circulations in Lake Biwa, part 1: model validation. *Limnology* **10**, 105–118.

Akitomo, K., Tanaka, K. & Kumagai, M. 2009b Annual cycle of circulations in Lake Biwa, part 2: mechanisms. *Limnology* **10**, 119–129.

Arhonditsis, G. B., Brett, M. T., DeGasperi, C. L. & Schindler, D. E. 2004 Effects of climatic variability on the thermal properties of Lake Washington. *Limnology and Oceanography* **49**, 256–270.

Beletsky, D., Hawley, N. & Rao, Y. R. 2013 Modeling summer circulation and thermal structure of Lake Erie. *Journal of Geophysical Research: Oceans* **118** (11), 6238–6252.

Bennington, V., McKinley, G. A., Kimura, N. & Wu, C. H. 2010 General circulation of Lake Superior: mean, variability, and trends from 1979 to 2006. *Journal of Geophysical Research: Oceans* **115** (C12), C12015.

Brooks, A. S. & Zastrow, J. C. 2002 The potential influence of climate change on offshore primary production in Lake Michigan. *Great Lakes Research* **28** (4), 597–607.

Chen, L., Gong, W., Zhang, H., Zhu, L. & Cheng, W. 2020 Lateral circulation and associated sediment transport in a convergent estuary. *Journal of Geophysical Research: Oceans* **125** (8), e2019JC015926.

Dipper, F. 2022 *Elements of Marine Ecology: Fifth Edition*. Elsevier, Amsterdam, Nederland.

Endoh, S., Okumura, Y. & Okamoto, I. 1995 Field observation in the North Basin. *Physical Processes in a Large Lake: Lake Biwa, Japan* **48**, 15–29.

Fer, I., Lemmin, U. & Thorpe, S. A. 2002 Observations of mixing near the sides of a deep lake in winter. *Limnology and Oceanography* **47** (2), 535–544.

Fischer, H. B., List, E. J., Koh, R. C. Y., Imberger, J. & Brooks, N. H. 1979 *Mixing in Inland and Coastal Waters*. Academic Press, New York, NY, USA.

Fofonoff, N. P. & Millard Jr., R. C. 1983 *Algorithms for the Computation of Fundamental Properties of Seawater*. UNESCO, Paris, France.

Haren, H. V. 2019 Internal wave mixing in warming Lake Grevelingen. *Estuarine, Coastal and Shelf Science* **226**, 106298.

Intergovernmental Panel on Climate Change (IPCC) 2021 *Climate change 2021: The physical science basis*. IPCC, Geneva, Switzerland. https://www.ipcc.ch/report/ar6/wg1/

Kitazawa, D., Kumagai, M. & Hasegawa, N. 2010 Effects of internal waves on dynamics of hypoxic waters in Lake Biwa. *Journal of the Korean Society for Marine Environmental Engineering* **13** (1), 30–42.

Koue, J. 2022 Evaluation of the impact of meteorological factors on the stratification of structure in Lake Biwa, Japan. *Hydrology* **9** (1), 16.

Koue, J., Shimadera, H., Matsuo, T. & Kondo, A. 2018 Evaluation of thermal stratification and flow field reproduced by a three-dimensional hydrodynamic model in Lake Biwa, Japan. *Water* **10** (1), 47.

Kumagai, M. & Vincent, W. F. 2003 *Freshwater Management: Global Versus Local Perspectives*. Springer-Verlag, Tokyo, Japan, pp. 1–22.

Kumagai, M., Robarts, R. D. & Aota, Y. 2021 Increasing benthic vent formation: a threat to Japan's ancient lake. *Scientific Reports* **11**, 4175.

Livingstone, D. M. 2008 A change of climate provokes a change of paradigm: taking leave of two tacit assumptions about physical lake forcing. *International Review of Hydrobiology* **93**, 404–414.

Morales-Mar'n, L. A., Wheater, H. S. & Lindenschmidt, K. E. 2017 Assessment of nutrient loadings of a large multipurpose prairie reservoir. *Journal of Hydrology* **550**, 66–185.

Munk, W. H. & Anderson, E. R. 1948 Notes on a theory of the thermocline. *Journal of Marine Research* **7**, 276–295.

Peeters, F., Livingstone, D. M., Goudsmit, G.-H., Kipfer, R. & Forster, R. 2002 Modeling 50 years of historical temperature profiles in a large central European lake. *Limnology and Oceanography* **47**, 186–197.

Rhodes, J., Hetzenauer, H., Frassl, M. A., Rothhaupt, K. & Rinke, K. 2017 Long-term development of hypolimnetic oxygen depletion rates in the large Lake Constance. *Ambio* **46** (5), 554–565.

Rueda, F. J., Vidal, J. & Schladow, G. 2009 Modeling the effect of size reduction on the stratification of a large wind-driven lake using an uncertainty-based approach. *Water Resources Research* **45**, W03411.

Saggio, A. & Imberger, J. 1998 Internal wave weather in a stratified lake. *Limnology and Oceanography* **43**, 1780–1795.

Shilo, E., Ashkenazy, Y., Rimmer, A., Assouline, S., Katsafados, P. & Mahrer, Y. 2007 Effect of wind variability on topographic waves: Lake Kinneret case. *Journal of Geophysical Research: Oceans* **112**, C12024.

Shimizu, K., Imberger, J. & Kumagai, M. 2007 Horizontal structure and excitation of primary motions in a strongly stratified lake. *Limnology and Oceanography* **52**, 2641–2655.

Shrestha, K. L. & Kondo, A. 2015 *Environmental Management of River Basin Ecosystems; Assessment of the Water Resource of the Yodo River Basin in Japan Using a Distributed Hydrological Model Coupled with WRF Model*. Springer, Berlin, Germany, pp. 137–160.

Stocker, R. & Imberger, J. 2003 Horizontal transport and dispersion in the surface layer of a medium-sized lake. *Limnology and Oceanography* **48** (3), 971–982.

Vincent, W. F., Gibbs, M. M. & Spigel, R. H. 1991 Eutrophication processes regulated by a plunging river inflow. *Hydrobiologia* **226**, 51–63.

Vinna, L. R., Medhaug, I., Schmid, M. & Bouffard, D. 2021 The vulnerability of lakes to climate change along an altitudinal gradient. *Communications Earth and Environment* **2**, 35.

Webb, E. K. 1970 Profile relationships: the log-linear range, and extension to strong stability. *Quarterly Journal of the Royal Meteorological Society* **96**, 67–90.

Woolway, R. I., Sharma, S., Weyhenmeyer, G. A., Debolskiy, A., Golub, M. & Jennings, E. 2021 Phenological shifts in lake stratification under climate change. *Nature Communications* **12**, 2318.

Yoshimizu, T., Yoshiyama, K., Tayasu, I., Koitabashi, T. & Nagata, T. 2010 Vulnerability of a large monomictic lake (Lake Biwa) to warm winter event. *Limnology* **11**, 233–239.